

# Improved phenomenological modelling of transient thermal strains for concrete at high temperatures

Claus V. Nielsen<sup>†</sup>

*Danish Technological Institute, P.O. Box 141, DK-2630 Taastrup, Denmark*

Chris J. Pearce<sup>‡</sup> and Nenad Bićanić<sup>‡†</sup>

*Department Civil Engineering, University of Glasgow, Rankine Building, Oakfield Avenue, Glasgow G12 8LT, U.K.*

*(Received September 15, 2003, Accepted March 31, 2004)*

**Abstract.** Several extensions to the Thelandersson phenomenological model for concrete under transient high temperatures are explored. These include novel expressions for the temperature degradation of the elastic modulus and the temperature dependency of the coefficient of the free thermal strain. Furthermore, a coefficient of thermo mechanical strain is proposed as a bi-linear function of temperature. Good qualitative agreement with various test results taken from the literature is demonstrated. Further extensions include the effects of plastic straining and temperature dependent Poisson's ratio. The models performance is illustrated on several simple benchmark problems under uniaxial and biaxial stress states.

**Keywords:** concrete; transient temperature effects; transient creep; load induced thermal strain; restraint stresses.

---

## 1. Introduction

### 1.1. Background

The behaviour of concrete is significantly altered when exposed to high temperatures. Mechanical properties such as strength and stiffness are generally found to be decreasing with temperature and high temperatures are found to significantly enhance the time dependent creep characteristics. Experimental evidence also suggests that strength, stiffness and creep depend on the combined load and temperature history, which needs to be included when concrete is to be modeled and analyzed under simultaneous loading and heating.

The temperature dependent behavior of concrete was summarized in the finishing document of the RILEM Technical Committee 44-PHT (Schneider 1986 and Schneider 1988), including most of the test data published on concrete subject to high temperatures until the mid eighties. Furthermore,

---

<sup>†</sup> Senior Consultant, Concrete Centre

<sup>‡</sup> Lecturer

<sup>‡†</sup> Regius Professor

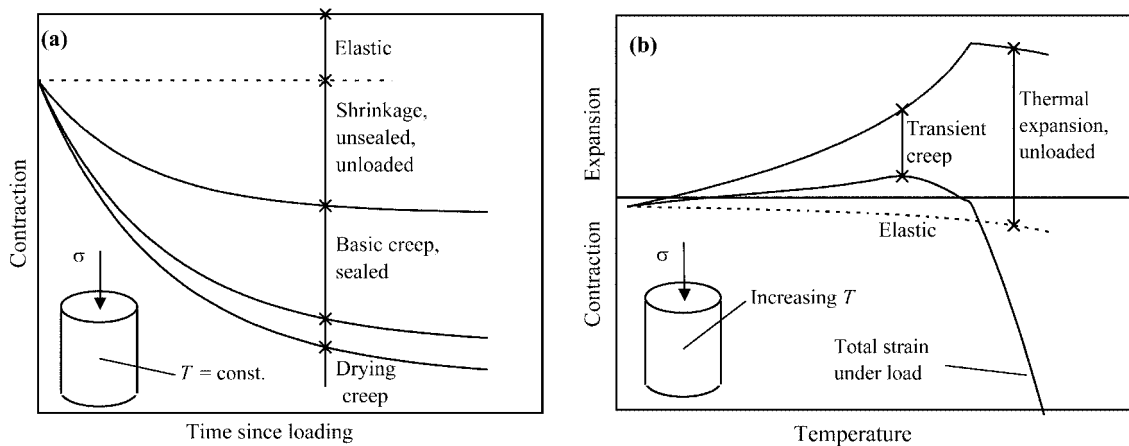


Fig. 1 Creep tests on concrete. (a) Creep strains vs. time under constant thermal and hygric environment, (b) Instantaneous transient strains vs. temperature during first time heating for unsealed conditions

Khoury, *et al.* (1985a) published a comprehensive review on the experimental evidence of transient creep of concrete and recently Bazant and Kaplan (1996) gave a thorough description of various aspects of concrete at high temperatures. At present, the RILEM Technical Committee 129-MHT continues the task of standardizing the procedures for high temperature tests on concrete and the notation and terminology of the present paper is largely in accordance with that applied by the recommendations published by TC 129-MHT (see e.g., RILEM 1998).

It is a well-documented fact that unsealed creep tests yield larger strains than the sum of the shrinkage and the basic creep strains (Fig. 1a) and the observed difference normally referred to as drying creep (Neville, *et al.* 1983) or 'stress induced shrinkage' (Bazant and Chern 1987). Heating of concrete specimens beyond 100°C under sealed conditions is very difficult to conduct (if not impossible) and thus, shrinkage of the cement paste is normally included in the test results. For an unloaded transient high temperature test the specimen undergoes thermal expansion. Performing the same test under sustained loading the total strains, excluding the elastic response, differ significantly from the unloaded situation (Fig. 1b). This difference is normally termed 'transient creep' or 'load induced thermal strain' and it is recognized to be much larger than the basic creep recorded under isothermal conditions (Fig. 1b). Furthermore, this strain component is found only for the first heating and it is considered as a quasi-instantaneous response closely connected with the change in temperature and moisture transport (Schneider 1986, Khoury, *et al.* 1985a, Thelandersson 1987).

Several investigations have dealt with the modeling of transient strains during combined heating and loading. Thelandersson (1982) and Schneider (1988) suggested uniaxial expressions for the transient creep, with the former applying the theory of plasticity and generalising the model to 3D. Khennane and Baker (1992, 1993) also adopted the theory of plasticity and based their numerical implementation on the work of de Borst and Peeters (1989). Thelandersson (1987) proposed a model, dividing the transient creep into viscous creep and thermo mechanical strain.

Bazant and Chern (1987) extended their original creep model to include the effect of temperature alterations, suggesting that both heating and cooling result in transient creep. Furthermore, the model by Bazant and Chern includes coupling of temperature and moisture fields, making it rather complex for practical design applications. Thienel and Rostasy (1996) proposed a general constitutive model for

transient strains, based on their own experimental biaxial results.

More recently, it has been recognised that the modelling of concrete at high temperatures calls for a consideration of the multiphase nature of the complex underlying processes which occur at different scales. On the macroscopic level, the coupling of thermo-mechanical formulations with mass transport has been undertaken by Bazant and Kaplan (1996), Gawin, *et al.* (1999), Tenchev, *et al.* (2001) and Khoury, *et al.* (2002) amongst others. The formulations consider moisture either as a single phase or treat the liquid and gas phases separately. Such formulations capture the build up of gas pressures due to rapid heating or as a result of sealed conditions and therefore enable a more realistic prediction of the effective stress. The effect of mechanical processes, such as cracking, on the heat and mass transport allows phenomena such as spalling to be modelled. A fully coupled hygro-thermal-mechanical approach obviously comes at a price, as the number of variables increases and the coupling becomes more involved.

Modelling of high temperature effects on the behaviour of concrete continues to be an active research area which increasingly considers the underlying physical and chemical mechanisms associated with temperature and humidity changes. Notable contributions include the microprestress-solidification theory (Bazant, *et al.* 2001) and the chemoplastic softening formulation (Ulm, *et al.* 1999) related to thermal hydration.

The authors believe that a multifield and multiscale setting for a constitutive model is ultimately necessary to rationally interpret and characterise the observed phenomena of concrete behaviour at high temperature. However, as the scientific debate is far from settled, authors also recognise a need for an improvement of the phenomenological constitutive models currently used in practice and the present paper represents a contribution in that context.

## *1.2. Scope of work*

The phenomenological constitutive models considered here are based on experimental data and the two models build on the work of Thelandersson and de Borst and Peeters and they do not explicitly consider the multiphysics nature of the underlying phenomena.

The investigation is meant to describe the main parameters recognized to affect transient strains of concrete in a simple and yet realistic manner and to illustrate their relative importance. The mechanical response of the concrete is kept linear and thus, the model is not meant to describe conditions close to failure. The implications of this assumption are discussed at the end of the article. Furthermore, it is noted that performance of the model is only validated experimentally against compressive test results since no tensile creep results exist to the authors knowledge.

## **2. Strain decomposition**

In the following sections a constitutive model for concrete subject to transient temperature and load scenarios is outlined. The model is a modification of the formulation given by Thelandersson (1987), applying experimental data of the load induced thermal strain (or transient creep) reported by Schneider (1986, 1988) and Khoury, *et al.* (1985a,b).

Thelandersson (1987) suggested an isotropic rheological model, comprising an elastic spring and a dashpot (Maxwell element) connected in series with a thermal expansion element and a thermo mechanical element. First the uniaxial case is considered, followed by a generalization to multiaxial conditions. The total uniaxial strain rate observed under first time heating is divided into the

following components

$$\dot{\varepsilon}_{tot}(T, \sigma) = \dot{\varepsilon}^{\sigma}(T, \sigma) + \dot{\varepsilon}_{th}(T) + \dot{\varepsilon}_c(T, \sigma) + \dot{\varepsilon}_{th}^{\sigma}(T, \sigma) \quad (1)$$

where dot denotes a derivative with respect to time. Temperature and stress are both unique functions of time ( $T=T(t)$  and  $\sigma=\sigma(t)$ ). Note that throughout the article the parentheses denoting the variables are only included when deemed necessary.

The four components in Eq. (1) are the mechanical strain rate  $\dot{\varepsilon}^{\sigma}$ , the free thermal strain rate  $\dot{\varepsilon}_{th}(T)$ , the creep strain rate  $\dot{\varepsilon}_c$  and the thermo mechanical strain rate  $\dot{\varepsilon}_{th}^{\sigma}$ . The last two terms comprise the load induced thermal strain rate (abbreviated lits by Khoury, *et al.* 1985b). The latter is recognized to appear only during first heating and not during subsequent cooling or heating cycles (Khoury, *et al.* 1985a). Thus, the load induced thermal strain represents an irrecoverable strain component that is crucial to the response of a concrete member subject to high temperatures since it may lead to severe tensile stresses during cooling (Nielsen, *et al.* 2002).

It is evident that one could add a shrinkage strain component to Eq. (1). However, since all experimental high temperature data are reported from unsealed test conditions the shrinkage component can be viewed as being included in the thermal strain. Furthermore, shrinkage is assumed to be independent of loading.

In the following sections each of the strain rate components of Eq. (1) is considered in turn and general expressions for the strain rates are given. For the purely mechanical component a novel expression for the temperature dependency of the elastic modulus is proposed. For the pure thermal strain an expression for the coefficient of thermal expansion is proposed to fit available experimental data. Finally, for the load induced thermal strain the existing models are assessed and the model by Thelandersson (1987) is modified such that the thermo mechanical parameters are fitted to existing experimental data. Furthermore, the assumption of neglecting the creep component  $\varepsilon_c$ , when interpreting transient creep test data, is justified by a simple example.

## 2.1. Mechanical strain

The mechanical strain may be split into an elastic and a plastic part  $\varepsilon^{\sigma} = \varepsilon_{el}^{\sigma} + \varepsilon_{pl}^{\sigma}$  (Schneider 1988, Khennane and Baker 1993). At present, only the elastic part is considered; however, issues related to the effect of including plastic mechanical strains are discussed later in the article.

Assuming  $\varepsilon^{\sigma}$  to form a surface in the stress-temperature space, the mechanical strain rate is obtained by applying the chain rule of differentiation:

$$\dot{\varepsilon}^{\sigma} = \frac{\partial \varepsilon^{\sigma}}{\partial \sigma} \dot{\sigma} + \frac{\partial \varepsilon^{\sigma}}{\partial T} \dot{T} \quad (2)$$

where  $\partial \varepsilon^{\sigma} / \partial \sigma = 1/E$  is the inverse slope of the stress-strain curve for a given temperature.

In the linear elastic case, where  $\varepsilon^{\sigma} = \varepsilon_{el}^{\sigma} = \sigma/E_{el}$ , the mechanical strain rate reads

$$\dot{\varepsilon}_{el}^{\sigma} = \frac{\dot{\sigma}}{E_{el}} + \left( \frac{1}{E_{el}} \right)' \dot{T} \sigma \quad (3)$$

where the prime denotes derivative with respect to temperature.

Experimental evidence shows that the modulus of elasticity degrades with increasing temperature (Schneider 1988, Bazant and Kaplan 1996). However, it is also recognized that the degradation is reduced when heating and compressive loading are applied simultaneously due to the closure of

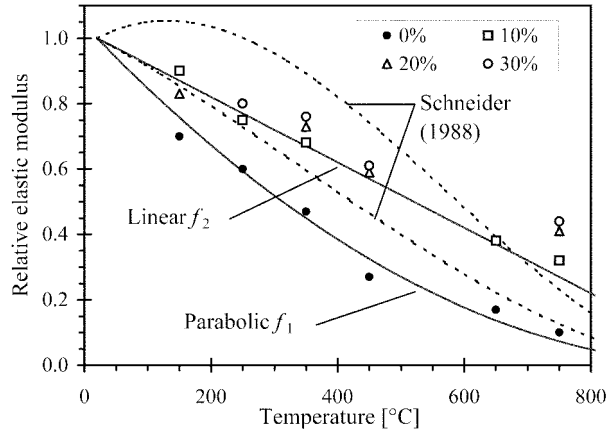


Fig. 2 Experimental data of  $E_{el}/E_0$  vs.  $T$  for various compressive stress levels (Schneider 1988). The legend figures give sustained compressive stress in percentage of  $f_c^0$ . The predictions by Schneider's model in Eq. (4) apply  $E_{el}/E_0 = g(T, \sigma)f_1(T)$  for  $\sigma$  equal to  $-0.1f_c^0$  and  $-0.3f_c^0$

micro cracks (Khoury, *et al.* 1985b, Schneider 1988). This sustained load effect introduces further complexities, as  $E_{el}$  becomes a function of both the stress history as well as temperature.

In Fig. 2 test data on normal concrete (Schneider 1988) are depicted together with analytical expressions for the temperature dependency of  $E_{el}$ . Schneider suggested the following expression for the elastic modulus

$$\frac{E_{el}(T, \sigma)}{E_0} = f(T)g(T, \sigma) \quad (4)$$

$$g(\theta(T), \sigma) = 1 - \frac{\sigma}{f_c^0}\theta, \quad \sigma \geq -0.3f_c^0$$

where  $E_0$ =elastic modulus at room temperature;  $f_c^0$ = compressive strength at room temperature;  $f$ = degradation function for unstressed conditions and  $\theta$  = dimensionless temperature defined by

$$\theta = \frac{T - T_0}{100^\circ\text{C}} \quad (5)$$

with  $T_0 = 20^\circ\text{C}$  (room temperature).

Schneider did not suggest a specific expression for  $f(T)$  needed in Eq. (4), however, a parabolic curve is found to be a plausible fit for the data in Fig. 2. Schneider's model in Eq. (4) is applied together for two different sustained stress levels (Fig. 2). It is seen that the experimental data does not support the pronounced effect of sustained stresses as implied by Eq. (4).

Instead of employing a stress dependency of  $E_{el}$  through the function  $g(T, \sigma)$ , a simple linear decreasing temperature dependency is suggested (Fig. 2). Thus, in case of unstressed heating  $E_{el} = f_1E_0$  and in case of sustained compressive stress  $E_{el} = f_2E_0$  with  $f_1$  and  $f_2$  given by

$$\left. \begin{aligned} f_1(\theta(T)) &= (1 - 0.1\theta)^2 \\ f_2(\theta(T)) &= 1 - 0.1\theta \end{aligned} \right\} 0 \leq \theta \leq 10 \quad (6)$$

Generalizing the uniaxial equation in (3) to the multiaxial case for an isotropic material the following

elastic strain rate is obtained

$$\dot{\epsilon}_{el,ij}^{\sigma} = \frac{1+\nu}{E_{el}} \dot{\sigma}_{ij} + \left(\frac{1+\nu}{E_{el}}\right)' \dot{T} \sigma_{ij} - \left[ \frac{\nu}{E_{el}} \dot{\sigma}_{kk} + \left(\frac{\nu}{E_{el}}\right)' \dot{T} \sigma_{kk} \right] \delta_{ij} \quad (7)$$

where the dots denote derivative with respect to time and the primes denote derivative with respect to temperature. Poisson’s ratio is first assumed to be independent of the temperature. Later on in the implications of this restriction are discussed and a temperature dependency of the Poisson’s ratio is introduced.

### 2.2. Free thermal strain

The free thermal strain of concrete is mainly influenced by the type and amount of the aggregate used. Its dependence on temperature is highly non-linear (Fig. 3), depending on the thermal stability of the aggregate. As previously mentioned the thermal strain may be decomposed into pure thermal strain, shrinkage strain and thermal damage strain. However, since testing at high temperatures is always performed under unsealed conditions, such decomposition is practically impossible and it can only be justified theoretically.

Here it is assumed that  $\epsilon_{th}$  is a function of temperature alone although several references suggest it depends on the heating rate as well. Hence, in case of high heating rates the chemical reactions and the moisture transport processes within the cement paste may not develop fully, affecting the thermal strain recordings.

The isotropic thermal strain rate reads

$$\dot{\epsilon}_{th,ij} = \alpha \dot{T} \delta_{ij} \quad (8)$$

where  $\alpha$  = coefficient of free thermal strain.

Nielsen, *et al.* (2002) suggested the coefficient  $\alpha$  for quartzite normal concrete is to be modeled by the following function

$$\alpha = \frac{0.06 \text{ ‰}}{7 - \theta \text{ }^{\circ}\text{C}}, \quad 0 \leq \theta \leq 6 \quad (9)$$

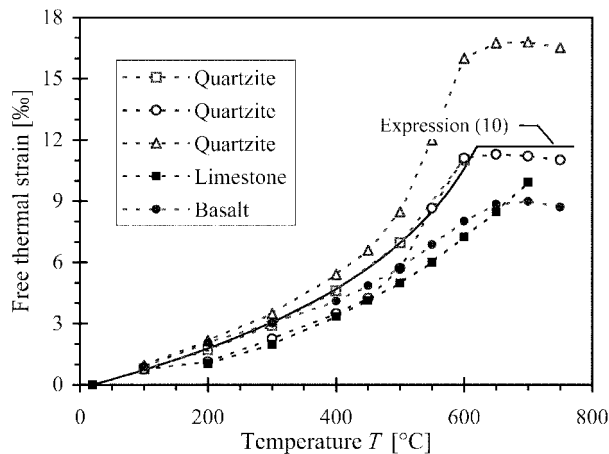


Fig. 3 Experimental  $\epsilon_{th}$  vs.  $T$  for various concretes. Solid line is analytical expression in Eq. (10)

meaning that the free thermal strain,  $\varepsilon_{th}$ , obtained during unrestrained heating from  $\theta = 0$  follows a logarithmic temperature dependency:

$$\varepsilon_{th} = -6\%_o \times \ln \left\{ 1 - \frac{\theta}{7} \right\} \quad (10)$$

In Fig. 3 this expression is compared with test data taken from Schneider (1986). Note that significant experimental variation in the thermal strain response exists, and therefore Eq. (10) is modeling a correct trend rather than closely fitting specific experimental values. It is seen how the experimental thermal strains level off when the temperature exceeds 600°C. Bazant and Kaplan (1996) suggested that this behavior is especially associated with quartzite aggregate, showing a significant increase in thermal strains between 500 and 600°C (due to the conversion of quartz crystals) where after the strain temperature curve flattens out. In the analytical expression this effect is obtained by a simple cut-off when  $\theta > 6$  in Eq. (10).

### 2.3. Load induced thermal strain

The load induced thermal strain, corresponding to the last two components in Eq. (1), is determined experimentally by measuring total strains during first time heating on a concrete specimen under sustained loading. The free thermal strain, recorded on an unstressed specimen, and the initial elastic strain are subtracted from the total strain to give the load induced thermal strain (or transient creep) as a function of temperature (Fig. 1b).

In the rheological model proposed by Thelandersson (1987) the load induced thermal strain rate in the uniaxial setting is given by

$$\dot{\varepsilon}_c + \dot{\varepsilon}_{th}^\sigma = \left( \frac{1}{\eta} + \frac{k}{f_c^0} \alpha \dot{T} \right) \sigma \quad (11)$$

where  $\eta$  = viscosity. The two terms on the right-hand-side correspond to a dashpot and a thermo mechanical element, respectively. The two components of the load induced thermal strain are termed temperature dependent creep and thermo mechanical strain, respectively. The viscosity is determined as a function of temperature level, stress level and time through an isothermal creep tests (steady-state load and temperature).

Thelandersson (1987) assumed a proportionality between the thermo mechanical strain  $\varepsilon_{th}^\sigma$  and the thermal strain  $\varepsilon_{th}$ , an assumption also adopted by others due to its simplicity (de Borst and Peeters 1989, Khennane and Baker 1993). Here this assumption is abandoned and a more general formulation is given.

As it is recognized that  $\varepsilon_c$  and  $\varepsilon_{th}^\sigma$  cannot be separated experimentally, the subdivision of the load induced thermal strain in two components is mainly theoretical and has little practical implications for short duration heating, as stated by Schneider (1988). However, one reason for the subdivision is that the two components have different characteristics, for instance the creep component takes place under both heating and cooling. Furthermore, such a subdivision shows creep recovery, whereas thermo mechanical strain is only experienced during first heating and not during subsequent cooling or heating.

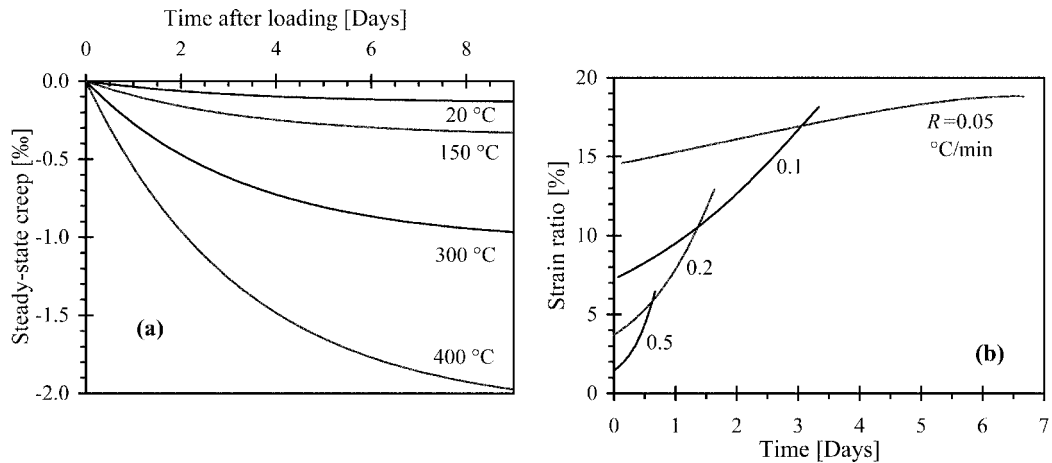


Fig. 4 Uniaxial member under sustained stress  $\sigma = -0.2f_c^0$ . (a) Examples of isothermal  $\varepsilon_{ssc}$  vs.  $t$  of normal quartzite concrete by means of Eq. (12). Sustained stress applied at  $t = 0$  after the indicated temperature level is reached and kept constant; (b) Examples of ratio  $\varepsilon_c / \varepsilon_{th}^\sigma$  vs.  $t$  for constant rate heating up to 500°C

### 2.3.1. Creep strain vs. thermo mechanical strain

The landersson (1987) stipulated that the creep strain  $\varepsilon_c$  is minor compared with  $\varepsilon_{th}^\sigma$  for practical test conditions even though steady-state creep is found to be enhanced by high temperatures (Fig. 4a). However, if the temperature increase is sufficiently slow the two components may be of a comparable magnitude. In the following a small analytical example is given to illustrate this point. It is justified that the conventional creep can be neglected when interpreting load induced test data by calculating the ratio  $\varepsilon_c / \varepsilon_{th}^\sigma$  for various heating rates (Fig. 4b).

The following analytical expression for the steady-state creep strain is proposed to fit test data for normal quartzite concrete tested under different temperature levels (Schneider 1986).

$$\varepsilon_{ssc} = 0.7\% \times \frac{\sigma}{f_c^0} e^{\theta/1.4} (1 - e^{-t/3.3\text{days}}) \quad (12)$$

where  $t$  = time since loading was applied,  $\sigma$  = constant compressive stress and  $\theta$  = dimensionless constant temperature according to Eq. (5). Eq. (12) is depicted in Fig. 4(a) for various temperatures.

By differentiating Eq. (12) with respect to  $t$ , the creep strain rate  $\sigma / \eta$  is found. Considering a test situation with sustained compressive stress ( $\sigma = \text{const.}$ ) during heating under a constant temperature rate  $R$ , one finds that time and temperature are related through  $Rt = 100^\circ\text{C} \times \theta$ . By integrating the creep strain rate  $\sigma / \eta$  with respect to time, the creep strain  $\varepsilon_c$  during the transient heating process is obtained. The thermo mechanical strain in Fig. 4(b) is calculated by means of  $\varepsilon_{th}^\sigma = k\sigma\varepsilon_{th} / f_c^0$  with  $k = 2.35$  (The landersson 1987) and  $\varepsilon_{th}$  given in Eq. (10).

Considering the slowest heating rate  $R = 0.05^\circ\text{C/min.}$ , (i.e., taking almost one week to reach 500°C), the creep strain to thermo mechanical strain ratio amounts to 15-20% and as the heating rate increases the ratio drops significantly. As practical experimental values of  $R$  are typically above  $1^\circ\text{C/min.}$  (Schneider (1986) reported  $2^\circ\text{C/min.}$ ), it seems plausible to assume that the creep component of the load induced thermal strain is neglected when interpreting the test results. Khoury, *et al.* (1985b) applied 0.2 and  $1^\circ\text{C/min.}$  and it is noted that the recommendations by RILEM TC

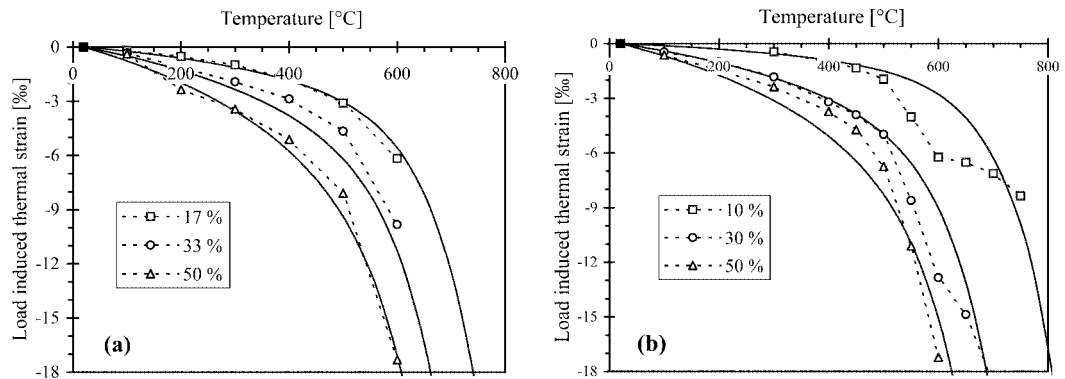


Fig. 5 Experimental data of load induced thermal strain for quartzite concrete taken from Schneider (1986). The legend figures give sustained compressive stress in percentage of  $f_c^0$ . The solid lines are the predictions by Schneiders model, applying  $f = f_1$  (see Eqs. (4) and (6))

129-MHT (1998) suggest a value as low as  $0.1^\circ\text{C}/\text{min}$ . for testing service conditions.

In the constitutive model presented in the following sections, the dashpot is therefore neglected in the expressions for the sake of simplicity. However, in case of long-term scenarios with loading and heating, the temperature dependent creep strain should of course be included in the calculations.

### 2.3.2. Experimental findings of load induced thermal strains in uniaxial compression

In the following, the terms ‘load induced thermal strain’ and ‘thermo mechanical strain’ are interchangeable (cf. previous section). Thus, it is assumed that the creep strain is negligible compared with the thermo mechanical strain under normal test conditions.

Schneider (1986) reported several test series of the load induced thermal strain of concrete tested under sustained uniaxial compressive load and a constant heating rate. The test series had been carried out at various laboratories throughout the 1970’s, see Schneider (1986) for details and references. Following the model by Schneider (1988) the uniaxial load induced thermal strain follows the expression (Fig. 5):

$$\varepsilon_{th}^{\sigma} = \frac{\sigma}{E_0} \frac{\phi + \frac{g-1}{f}}{g} \quad (13)$$

$$\phi = C_1 \tanh c_1 \theta + C_2 (\tanh c_2 (\theta - \theta_g) + 1)$$

where  $f$  and  $g$  are identical to those defined earlier in Eq. (4) and  $\phi$  is a function of temperature with the following parameters given by Schneider (1988)  $C_1 = 2.6$ ;  $c_1 = 0.28$ ;  $c_2 = 0.75$ ;  $\theta_g = 6.8$  and  $C_2 = 1.4$  for quartzite aggregate. Schneider (1988) also suggests parameters for limestone concrete (Fig. 6).

During the 1980s extensive experimental research took place at the Imperial College in London. The tests included transient creep for various concretes up to  $600^\circ\text{C}$  (Khoury, *et al.* 1985a,b). Khoury, *et al.* suggested the existence of a master curve of load induced thermal strain, assumed to be largely independent of aggregate type, concrete strength, age and initial moisture content.

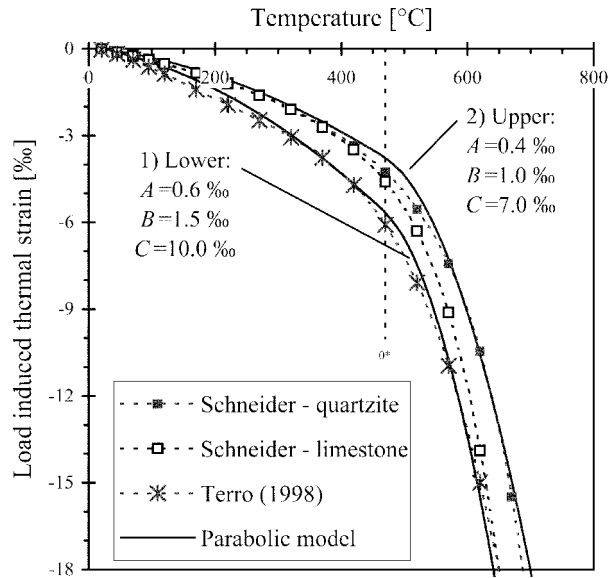


Fig. 6 Comparison between uniaxial  $\varepsilon_{th}^{\sigma}$  vs.  $T$  modeled by Schneider (1988) and Terro (1998) for  $\sigma = -0.3 f_c^0$ . Upper and lower bounds of the parabolic model from Eq. (17), proposed in the present article, is also depicted

Furthermore, the test results of Khoury, *et al.* did not confirm the simple proportionality between  $\varepsilon_{th}^{\sigma}$  and  $\varepsilon_{th}$ , as proposed by Thelandersson (1987), which is not entirely surprising since thermal strain is strongly related to the aggregate while thermo mechanical strain is mainly associated with the cement paste.

Recently Terro (1998) applied a fourth order polynomial to fit this master curve based on the Imperial College data. The expressions by Terro and Schneider are compared in Fig. 6.

Generally it is found that the results of Khoury, *et al.* (1985b) (analytically modeled by Terro 1998) yield numerically larger values of load induced thermal strains for a given temperature than those of Schneider (1986). Beside the differences in test equipment, test procedures and concrete mix, this trend is partly explained by the fact that the former tests were performed at a lower heating rate than the latter. Hence, the time dependent effects (shrinkage, creep, etc.) become more significant.

### 3. Model A - Thermo mechanical strain model

The general formulation of the thermo mechanical strain rate by Thelandersson (1987) reads

$$\dot{\varepsilon}_{th,ij}^{\sigma} = (\gamma_1 \sigma_{kk} \delta_{ij} + \gamma_2 \sigma_{ij}) \dot{T} \quad (14)$$

where two coefficients of thermo mechanical strain,  $\gamma_1$  and  $\gamma_2$ , to be determined experimentally, are introduced. Comparing Eq. (14) and Eq. (11) it is seen that the sum  $\gamma_1 + \gamma_2$  governs the uniaxial behavior with  $\gamma_1 + \gamma_2 = k\alpha / f_c^0$ .

A clearer physical understanding is achieved by applying the following substitutions similar to those suggested by de Borst and Peeters (1989):

$$\gamma_1 = -\nu_c \frac{\beta}{f_c^0}, \quad \gamma_2 = (1 + \nu_c) \frac{\beta}{f_c^0} \quad (15)$$

where  $\nu_c$  = transient creep Poisson's ratio and  $\beta$  = coefficient of uniaxial thermo mechanical strain. Inserting in Eq. (14) yields

$$\dot{\varepsilon}_{th,ij}^{\sigma} = -\beta \left( \nu_c \frac{\sigma_{kk}}{f_c^0} \delta_{ij} - (1 + \nu_c) \frac{\sigma_{ij}}{f_c^0} \right) \dot{T} \quad (16)$$

It is seen that  $\nu_c$  is analogous to the elastic Poisson's ratio. There is experimental body of evidence that conventional creep has a lateral component similar to elastic strains (Gopalakrishnan, *et al.* 1969 and Neville *et al.* 1983). Hence, subjecting concrete to uniaxial sustained compression, the axial creep (contraction) is accompanied by lateral expansion. It can be argued that the experimental findings of the magnitude of the lateral creep are highly inconclusive with the creep Poisson's ratio ranging from zero to values equal to the elastic Poisson's ratio. Neville, *et al.* (1983) suggested that the differences were mainly due to different test conditions and especially the presence of drying creep. However, the magnitude of a creep Poisson's ratio is similar to the elastic ratio.

To the authors knowledge the bulk of experiments on load induced thermal strain did not include lateral deformation measurements so that not much information is available on  $\nu_c$ . However, the experiments of Ehm (1986) showed that load induced thermal strains have a lateral component similar with that observed in conventional creep tests.

In the uniaxial setting, the product  $\beta\sigma/f_c^0$  represents the slope of the relation between  $\varepsilon_{th}^{\sigma}$  vs.  $T$  (Figs. 5 and 6). Here the parabolic temperature dependency is suggested for the uniaxial thermo mechanical strain

$$\varepsilon_{th}^{\sigma} = \frac{\sigma}{f_c^0} y \quad (17)$$

$$y = \begin{cases} A\theta^2 + B\theta, & 0 \leq \theta \leq \theta^* = 4.5 \\ C(\theta - \theta^*)^2 + A(2\theta - \theta^*)\theta^* + B\theta, & \theta^* < \theta \end{cases}$$

where  $\theta^*$  = dimensionless transition temperature between the two expressions (470°C). The reason for applying a combination of two parabolic expressions (with a common tangent at the transition temperature) instead of following Terro (1998) who applied a fourth order polynomial expression is to better capture the rather abrupt change in behavior experimentally detected around the transition temperature (Fig. 5). Furthermore, the parabolic model keeps the formulation simple with  $A$  and  $B$  governing the initial part and  $C$  the subsequent part of the  $\varepsilon_{th}^{\sigma}-\theta$  relationship. No attempt is made here to speculate on the underlying reasons for the observed abrupt change at the transition temperature  $\theta^*$ .

The simplicity of the model is also maintained by applying a direct proportionality with the stress level unlike Schneider's model where  $\varepsilon_{th}^{\sigma}$  is a non-linear function of  $\sigma$ , cf. Eqs. (13) and (4). The assumption of direct proportionality with the stress level is supported by experiments (Khoury, *et al.* 1985b, Thienel 1993).

It is seen that the parabolic model captures the experimental behavior in a satisfactory manner (Fig. 6). The two sets of parameters ( $A, B, C$ ) applied in Fig. 6 describe an upper and a lower curve. The former agrees best with the experimental data presented by Schneider (1986) and the latter is more in correspondence with the master curve by Khoury, *et al.* (1985b) and Terro (1998). The difference between the two curves was discussed in terms of time dependent effects in a

previous section. Thus, the two limiting parabolic curves in Fig. 6 define a range where the thermo mechanical strain is likely to be found for normal concretes with various aggregate types.

Finally, by calculating the slope  $\partial \varepsilon_{th}^{\sigma} / \partial T = \beta \sigma / f_c^0$  from Eqs. (17), the temperature dependent coefficient of uniaxial thermal strain  $\beta$  is found as a bi-linear function of temperature:

$$\beta = y' = \theta' \times \begin{cases} 2A\theta + B, & 0 \leq \theta \leq \theta^* \\ 2C(\theta - \theta^*) + 2A\theta^* + B, & \theta^* < \theta \end{cases} \quad (18)$$

where prime denotes a derivative with respect to temperature, i.e.,  $\theta' = 1/(100^\circ\text{C})$ .

### 3.1. Model A - Benchmark problems

The full 3D generalisation of the constitutive model reads  $\dot{\varepsilon}_{tot,ij} = \dot{\varepsilon}_{el,ij} + \dot{\varepsilon}_{th,ij} + \dot{\varepsilon}_{th,ij}^{\sigma}$  with the strain rates defined in Eqs. (7), (8) and (16), respectively.

$$\begin{aligned} \dot{\varepsilon}_{el,ij}^{\sigma} &= \frac{1+\nu}{E_{el}} \dot{\sigma}_{ij} + \left( \frac{1+\nu}{E_{el}} \right)' \dot{T} \sigma_{ij} - \left[ \frac{\nu}{E_{el}} \dot{\sigma}_{kk} + \left( \frac{\nu}{E_{el}} \right)' \dot{T} \sigma_{kk} \right] \delta_{ij} \\ \dot{\varepsilon}_{th,ij}^{\sigma} &= \alpha \dot{T} \delta_{ij} \\ \dot{\varepsilon}_{th,ij}^{\sigma} &= -\beta \left( \nu_c \frac{\sigma_{kk}}{f_c^0} \delta_{ij} - (1 + \nu_c) \frac{\sigma_{ij}}{f_c^0} \right) \dot{T} \end{aligned} \quad (19)$$

where the dots and the primes denote derivative with respect to  $t$  and  $T$ , respectively. In the following sections the model performance is illustrated in a parameter study on several model problems.

#### 3.1.1. Case I - Uniaxial restraining test

In order to evaluate how the model performs with realistic material behavior an example is given of a uniaxial concrete member subject to constant rate heating when fully restrained against expansion. All stresses are zero except  $\sigma_{11} = \sigma$  and the axial strain  $\varepsilon_{tot,11}$  is kept constant. Applying the dimensionless parameters for stress,  $s = \sigma / f_c^0$ , and time,  $\tau = Rt / T_0$ , the first order differential equation to be solved with respect to  $s$  is obtained

$$\frac{d\varepsilon_{tot,11}}{d\tau} = \frac{f_c^0}{E_{el}} \frac{ds}{d\tau} + \alpha T_0 + \left( \beta T_0 + \frac{d}{d\tau} \left( \frac{f_c^0}{E_{el}} \right) \right) s = 0 \quad (20)$$

where the dimensionless relation between time and temperature is  $(100^\circ\text{C})\theta = \tau T_0$ , leading to the

Table 1 Input parameters for Fig. 7. See Eq. (6) for  $f_2$

Curve no.	$s(0)$	$A, B, C$ [%]	$E_{el}/E_0$
1	0	0.6, 1.5, 10.0	$f_2$
2	0	0.4, 1.0, 7.0	$f_2$
3	0	0.4, 1.0, 7.0	1
4	-0.3	0.4, 1.0, 7.0	$f_2$
5	0	0, 0, 0	$f_2$

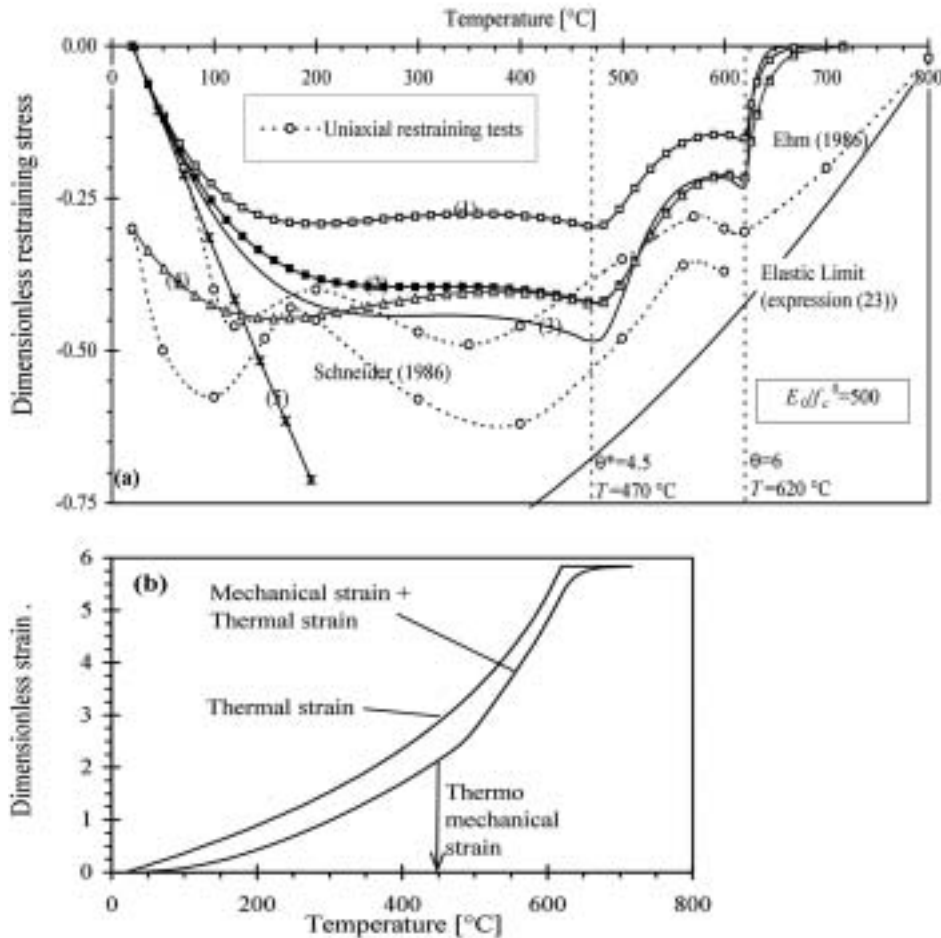


Fig. 7 Uniaxial restraining test. (a) Parameter study of (20) with parameters given in Table 1. Test results taken from Schneider (1986) and Ehm (1986) for normal quartzite concrete (air cured). (b) Strains divided by  $f_c^0 / E_0$  for curve 2

following identity,  $T_0(d/dT) = d/d\tau$ . The parameters  $\alpha$ ,  $\beta$ , and  $E_{el}$  are variables depending on temperature, described by Eqs. (9), (18) and (6), respectively.

The differential Eq. (20) with a prescribed initial condition is solved numerically for various input parameters (Table 1, Fig. 7). Curves 1 and 2 depict the influence of the two limiting parabolic curves suggested in Fig. 6. It is obvious that the adopted  $\beta$  model has a great influence on the result. Curves 2 and 3 depict the influence of taking the stiffness degradation into account. It is seen that neglecting the degradation and keeping  $E_{el} = E_0$  throughout the heating, a less significant effect is obtained compared with the effect of the specific choice of  $\beta$  model mentioned earlier. Curve 4 has material parameters identical with curve 2 but with an initial prestress applied. Finally, curve 5 shows how the restraining stress would increase rapidly and crush the sample if no thermo mechanical strain effect is taken into account, i.e., for  $\beta = 0$  in Eq. (20).

The vertical dotted lines in Fig. 7(a) indicate distinct changes occurring in the material properties: the first change at  $\theta = \theta^* = 4.5$  corresponds to the transition temperature of the bi-linear expression

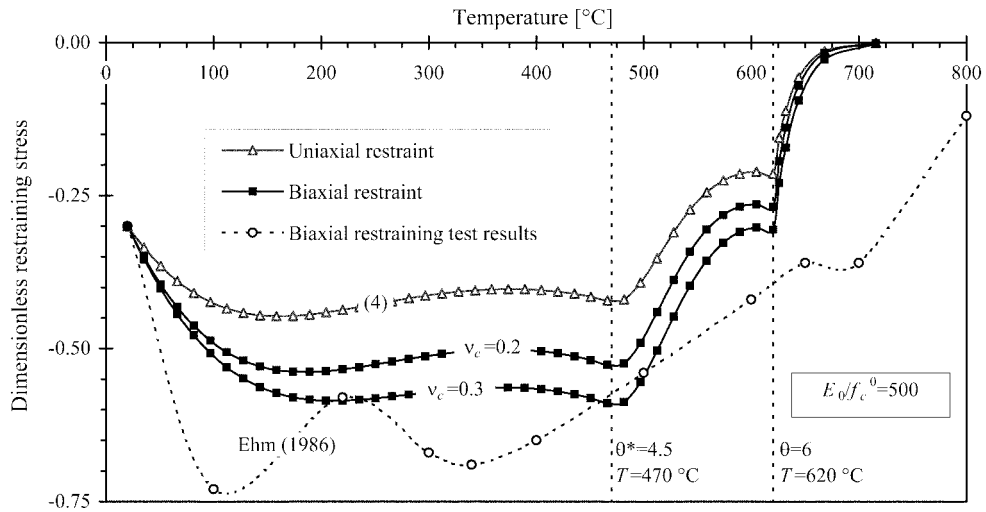


Fig. 8 Symmetric biaxial restraining test. Example of numerical solution of Eq. (21) with model parameters identical to curve 4 (Table 1), constant elastic Poisson's ratio  $\nu = 0.2$  and two constant values of  $\nu_c$ . Biaxial and uniaxial test results from Ehm (1986) for normal quartzite concrete (air cured)

for  $\beta$  in Eq. (18), while the second change at  $\theta = 6$  corresponds to the abrupt change of the coefficient of free thermal strain (Fig. 3).

Experimentally observed restraint stresses, recorded for the case of  $2^\circ\text{C}$  per minute heating of uniaxially restrained concrete specimens, are taken from Ehm (1986) for the zero initial stress case and Schneider (1986) for the 30% initial prestress case (Fig. 7a).

It should be noted that the adopted model parameters are based on an indication of a general trend and are not fitted to match any particular set of test results. Both relationships for  $\alpha$  and  $\beta$  follow general expressions, not necessarily tuned to fit with the characteristics of the specific concrete mix used in the tests. Nevertheless, it is clear that the proposed model qualitatively captures the experimental behavior, although the experimental stress peaks are more pronounced and shifted along the temperature axis compared with the model predictions. This is especially true in the beginning, where the model does not predict the build-up of stresses quickly enough, indicating that the value of  $\alpha$  may be too small relative to  $\beta$  for temperatures below  $100^\circ\text{C}$ . This may be connected with the fact that hygral effects, which are known to be strong in the temperature range up to  $200^\circ\text{C}$ , are not included in the present model. De Borst and Peeters (1989) and Khennane and Baker (1993) also reported and discussed this discrepancy.

The axial strain components for curve 2 (divided by the elastic strain  $f_c^0/E_0$ ) are depicted in Fig. 7(b). The thermo mechanical strain, which is irreversible, is equal to the negative sum of the free thermal strain and the elastic strain. The latter is illustrated as the difference between the two curves in Fig. 7(b). It is seen how the irreversible strain is significant in magnitude compared with the elastic strain during heating.

### 3.1.2. Case II - Biaxial restraining test

During a symmetric biaxial restraining test with  $\sigma_{11} = \sigma_{22} = \sigma$  and all other stresses set to zero the dimensionless first order differential equation, derived analogous to Eq. (20), reads

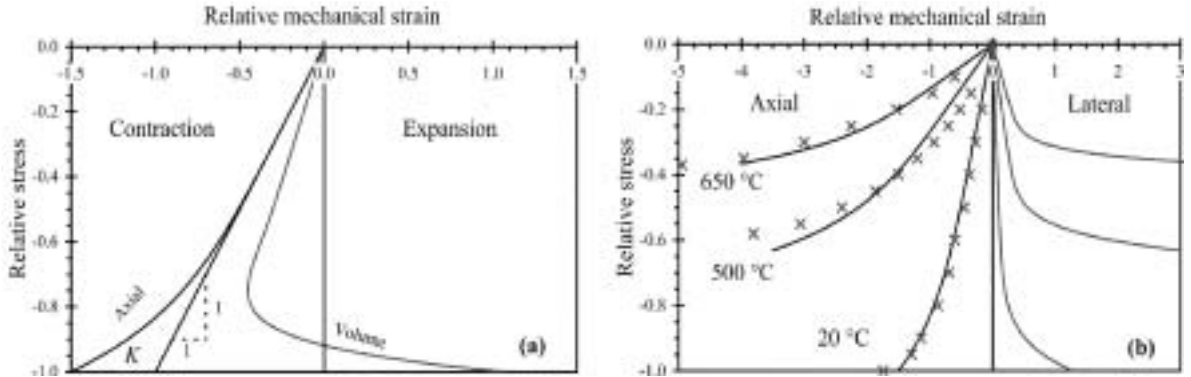


Fig. 9 Non-linear uniaxial stress - strain curves. (a)  $\sigma/f_c^T$  vs.  $E_{el}\epsilon^\sigma/f_c^T$  and corresponding volumetric strain. (b)  $\sigma/f_c^0$  vs.  $E_0\epsilon^\sigma/f_c^0$  and corresponding lateral strains. The crosses are experimental axial stress strain data for Thelanderssons quartzite concrete (taken from Schneider 1986)

$$\frac{d\epsilon_{tot,11}}{d\tau} = (1 - \nu) \frac{f_c^0}{E_{el}} \frac{ds}{d\tau} + \alpha T_0 + \left( (1 - \nu_c) \beta T_0 + \frac{d}{d\tau} \left( (1 - \nu) \frac{f_c^0}{E_{el}} \right) \right) s = 0 \quad (21)$$

Examples of the numerical solution to Eq. (21) for constant values of the Poisson's ratio are presented in Fig. 8 and compared with test data taken from Ehm (1986) and the uniaxial restraint curve 4 from Fig. 7(a). Ehm (1986) reported that the elastic Poisson's ratio increases slightly with temperature, which appears to be in contradiction with earlier experimental findings (Schneider 1986 and Bazant and Kaplan 1996). Due to these inconclusive findings and the fact that the elastic strains are of minor significance compared with the thermal strain components, a constant Poisson's ratio is adopted. Fig. 8 shows how the model captures the important response characteristics even with Poisson's ratio kept constant throughout the temperature range.

#### 4. Model B - Thermo mechanical strain model including the effects of plastic strains and temperature dependent Poisson's ratio

In the previous sections restraining stresses have been calculated with realistic temperature dependent material properties. However, in order to maintain simplicity the non-linear stress strain curve of concrete, variation in the Poisson's ratio was neglected. In the present section these issues are discussed and the model is extended to include these features. However, the need for further experiments in order to validate the effect of especially Poisson's ratio is evident.

Schneider (1988) introduced a relatively simple power law to model the nonlinear, temperature dependent uniaxial compressive stress - strain relationship (Fig. 9a) for normal strength concrete:

$$\begin{aligned} \epsilon^\sigma &= \epsilon_{el}^\sigma + \epsilon_{pl}^\sigma = \frac{\sigma}{E_{el}(T)} (1 + K(T, \sigma)) \\ K &= -\frac{1}{2} \left( \frac{\sigma}{f_c^T} \right)^5, \quad -f_c^T \leq \sigma \leq 0 \end{aligned} \quad (22)$$

where  $K$  = plastic to elastic strain ratio;  $f_c^T$  = temperature dependent compressive strength and  $E_{el}$  = temperature dependent elastic modulus. If Schneider's proposal is interpreted as an elastoplastic model, it is seen that the model implies that the plastic strain at peak stress is equal to 50% of the

corresponding elastic strain, and furthermore, the stress - strain curves does not exhibit a horizontal tangent at peak stress. Despite these limitations the model is deemed appropriate for the present purpose (Fig. 9b). It is noted that Khennane and Baker (1993) applied a more complex model where the evolution of plastic strains is assumed to follow a different expression. The temperature dependent compressive strength is assumed to follow a parabolic expression

$$\frac{f_c^T}{f_c^0} = 1 - 0.016\theta^2, \quad 0 \leq \theta \leq 7.9 \quad (23)$$

By knowing how strength decreases with temperature allows for the evaluation of the so-called critical temperature for a given sustained stress. Schneider (1986) defined the critical temperature as the temperature at which the specimen fails during heating (i.e., the temperature fulfilling the equation  $\sigma = -f_c^T$  with constant  $\sigma$ ). Schneider reported that for normal concrete the critical temperature decreases very rapidly from about 500 to 100°C when compressive stress levels exceed 70 to 80% of  $f_c^0$ . Thus, for stress levels of this magnitude the interpretation of thermo mechanical test data is complicated by the fact that the specimen may start to fail as a result of reaching the critical temperature.

Furthermore, it is a well-known experimental fact that when the stress approaches the concrete strength a significant lateral strain develops, making the volume strains shift from contraction to dilation (Fig. 9a). This shift appears to happen at stress levels around 75 to 85% of the ultimate strength. This effect is modeled by assuming the elastic Poisson's ratio to be constant and equal to 0.2 below the stress proportionality limit, i.e., for  $0 \geq \sigma \geq -0.5 f_c^T$ . Beyond the proportionality limit Poisson's ratio,  $\nu$  is both temperature and stress dependent, expressed through the third order polynomial.

$$\nu(T, \sigma) = 0.2 - \left[ 25.6 \left( \frac{\sigma}{f_c^T} + 0.5 \right) + 1.6 \right] \left( \frac{\sigma}{f_c^T} + 0.5 \right)^2 \quad (24)$$

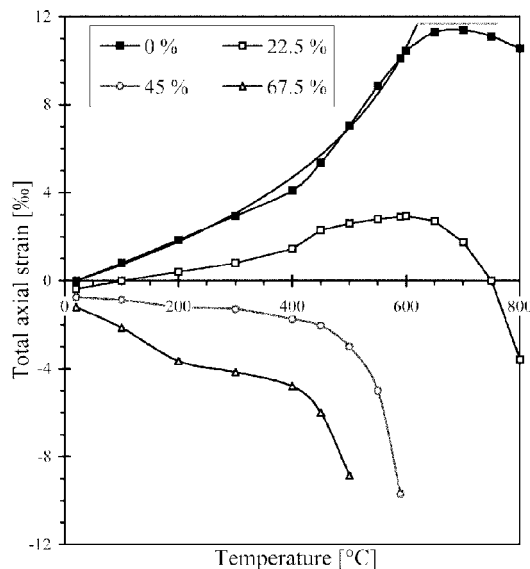


Fig. 10 Experimental total strains from transient tests (Thelandersson 1987). The legend figures are sustained compressive stress in percentage of  $f_c^0$ . Solid line is the free thermal strain by means of Eq. (10)

where the valid stress range is  $-0.5 f_c^T \geq \sigma \geq -f_c^T$ . Note that the elastic Poisson's ratio is defined as the negative ratio between the lateral and the axial mechanical strain rate. Eq. (24) is arranged so that the value of  $\nu=0.5$  is reached for  $\sigma=-0.75 f_c^T$ , corresponding to the point where the volumetric strain in Fig. 9(a) shifts to dilation.

In Fig. 9(b) it is seen how Eqs. (22)-(24) govern the uniaxial compressive behavior, applying  $E_{el} = f_1 E_0$ . Furthermore, the agreement with experimental uniaxial stress - strain curves, obtained under isothermal conditions, is noted.

The uniaxial mechanical strain rate is now obtained by inserting Eq. (22) in Eq. (2)

$$\dot{\varepsilon}^\sigma = \frac{\dot{\sigma}}{E_{el}}(1 + 6K) + \left( \left( \frac{1}{E_{el}} \right)' (1 + K) + 5K \frac{f_c^T}{E_{el}} \left( \frac{1}{f_c^T} \right)' \right) \sigma \dot{T} \quad (25)$$

where dot and prime again denote derivatives with respect to  $t$  and  $T$ , respectively, and the following derivatives have been applied

$$\begin{aligned} \frac{\partial}{\partial \sigma} \sigma K &= 6K \\ \frac{\partial}{\partial T} \frac{1 + K}{E_{el}} &= \left( \frac{1}{E_{el}} \right)' (1 + K) + 5K \frac{f_c^T}{E_{el}} \left( \frac{1}{f_c^T} \right)' \end{aligned} \quad (26)$$

The lateral strain rate is obtained by multiplying Eq. (25) with  $-\nu$ . The thermal strain rate and the thermo mechanical strain rate are both identical to the formulations in the previous sections.

#### *4.1. Comparison of model A and B with uniaxial test results*

In the following the transient tests data reported by Thelandersson (1987) are reproduced by means of the proposed model B predictions, including the plastic mechanical strains and the stress and temperature dependent Poisson's ratio. The tests consisted of concrete cylinders subject to sustained stress and constant rate heating, see total strain recordings in Fig. 10. It is noted that the model predictions for the free thermal strain (10) fit Thelandersson's experimental data remarkably well.

Fig. 11 shows the total strain data from Fig. 10 together with the model B predictions including the effect of mechanical plastic strains and temperature dependent Poisson's ratio. Furthermore, the total strains from model A are also depicted (i.e., omitting the plastic mechanical strains and keeping the Poisson's ratios constant).

In order to maintain simplicity the transient creep Poisson's ratio is kept identical to the elastic Poisson's ratio ( $\nu = \nu_e$ ) for all the calculations. Note also that Fig. 11 depicts both axial and lateral strain predictions, while only the former is reported experimentally.

It is seen how the total strains are captured in a satisfactory manner (Fig. 11). Only for the lowest load level (Fig. 11a) the difference between the experiments and the model prediction is substantial, which is mainly due to the critical temperature being predicted at about 710°C by Eq. (23) whereas the critical temperature is experimentally found to be around 800°C. The effect of including the plastic mechanical strains following Eq. (22) is found to be insignificant compared with the thermal and the thermo mechanical strains.

However, the effect of including the temperature dependency of the Poisson's ratio is significant

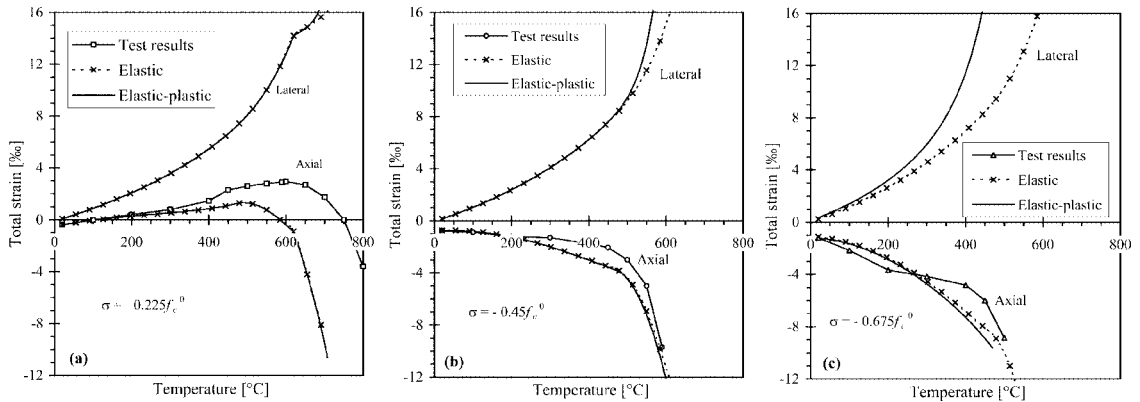


Fig. 11 Experimental total strains vs. temperature. The broken lines with crosses represent calculations without plastic mechanical strains, applying constant  $\nu = \nu_c = 0.2$ . The solid lines include plastic mechanical strains and Poisson's ratio  $\nu_c = \nu(T, \sigma)$ . Parameters are  $(A, B, C) = (0.6, 1.5, 10.0) \%$ ,  $E_0 / f_c^0 = 600$  and  $E_{el} = f_2 E_0$

for the lateral strains and the effect increases with the magnitude of the compressive stress level. This is further illustrated in Fig. 12 where the model predictions of the volumetric thermo mechanical strains are depicted. First the concrete specimen undergoes contraction followed by a significant dilation when the critical temperature is approached. If instead Poisson's ratio is maintained constant (model A) the volumetric contraction will continue to increase as indicated by the dotted line in Fig. 12(a). By comparing with normal concrete results reported by Ehm (1986) in Fig. 12(b) it is clear that this shift in volume strains from contraction to dilation is evident both in uniaxial and biaxial tests (this was also reported by Thienel 1993).

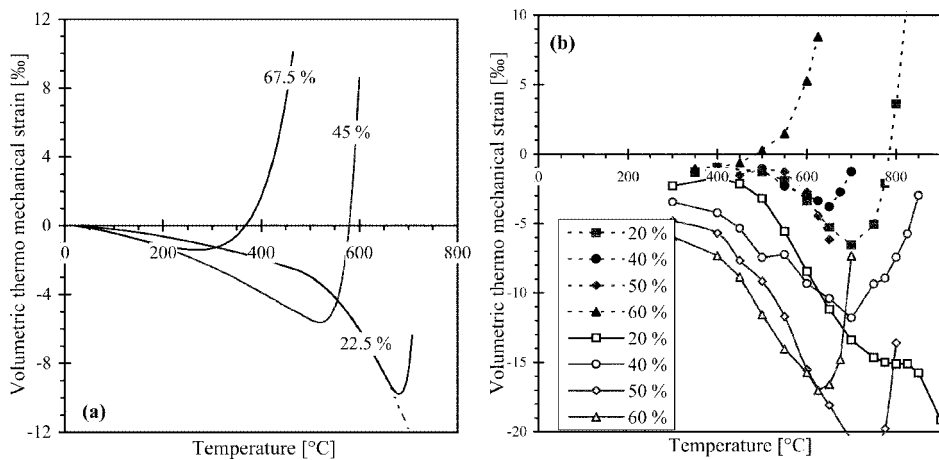


Fig. 12 Volumetric thermo mechanical strains for sustained uniaxial stress during heating. The legend figures are sustained compressive stress in percentage of  $f_c^0$ . (a) Model predictions from the calculations in Fig. 11, including plastic mechanical strains and temperature dependent Poisson's ratio. (b) Test data from Ehm (1986). Filled symbols: uniaxial tests; open symbols: symmetric biaxial tests

## 5. Conclusions

Strains in concrete under transient high temperatures are recognised to be irreversible during first heating. The proposed constitutive model is based on a modified rheological model suggested by Thelandersson (1987). The total strain under transient conditions is decomposed into pure mechanical strain, free thermal strain and load induced thermal strain. The latter, often being termed transient creep, is decomposed into conventional creep (temperature dependent) and a combined thermo mechanical strain. It is demonstrated how the latter is much larger than the former under most conditions.

The thermo mechanical strain is considered irreversible and it occurs only during first heating due to the combination of stress and temperature increase. During heating these strains help relax the stresses arising from thermal gradients and incompatibilities between the aggregate and the cement paste. However, the irreversibility of the thermo mechanical strain leads to the build up of tensile restraint stresses during cooling (Nielsen, *et al.* 2002).

Instead of assuming direct proportionality between the free thermal strain and the thermo mechanical strain (as suggested by Thelandersson 1987) a separate thermo mechanical coefficient  $\beta$  is proposed. Moreover, the model introduces a parabolic expression to describe the uniaxial thermo mechanical response where  $\beta$  becomes a bi-linear function of temperature. Finally, a transient creep Poissons ratio is introduced to describe the corresponding lateral thermo mechanical response.

Model A performance is illustrated by two simple examples where uniaxial and biaxial restraint conditions are modeled. Qualitative agreement with experimental data is demonstrated. Model B incorporates the effect of plastic mechanical strains and temperature dependent Poisson's ratio. The effect is found to be of importance when the stress is close to the ultimate strength of the material, i.e, the temperature level is close to the critical temperature. It is believed that for most applications the inclusion of elastic mechanical strains only (model A) will be adequate.

Finally, it is realized that more experimental data is needed both under uniaxial conditions (including recordings of axial as well as lateral strains) and especially under multiaxial conditions. Also the thermo mechanical response in tension is still to be investigated experimentally.

## Acknowledgements

This work was carried out during the first authors Marie Curie Fellowship funded by the European Commission under FP5, the Fifth Framework Programme (contract no. HPMF-CT-1999-0171).

## References

- Bazant, Z. P. and Chern, J. C. (1987), "Stress-induced thermal and shrinkage strains in concrete", *J. Eng. Mech.*, ASCE, **113**(10), 1493-1511.
- Bazant, Z. P. and Kaplan, M. F. (1996), "Concrete at high temperatures, Material properties and mathematical models", Longman Group Ltd., Essex, England.
- Bazant, Z. P., Cedolin, L. and Cusatis, G. (2001), "Temperature effect on concrete creep modeled by microprestress-solidification theory", *Creep, Shrinkage and Durability Mechanics of Concrete and Other Quasi-Brittle Materials (Proceedings 6<sup>th</sup> International Conference, CONCREEP-6)*, F.-J. Ulm, Z. P. Bazant and F. H. Wittmann, eds., Elsevier, Amsterdam. 197-204.
- de Borst, R. and Peeters, P.P.J.M. (1989), "Analysis of concrete structures under thermal loading", *Comp. Meth. Appl. Mech. Eng.*, **77**, 293-310.
- Ehm, C. (1986), "Versuche zur Festigkeit und Verformung von Beton unter zweiachialer Beanspruchung und

- hohen Temperaturen”, PhD thesis, Heft 71, IBMB, Technical University of Braunschweig, Braunschweig, Germany (in German).
- Gawin, D., Majorana, C. E. and Schrefler, B.A. (1999), “Numerical analysis of hygro-thermal behaviour and damage of concrete at high temperature”, *Mech. Cohes.-Frict. Mater.*, **4**, 37-74.
- Gopalakrishnan, K. S., Neville, A. M. and Ghali, A. (1969), “Creep Poisson’s ratio of concrete under multiaxial compression”, *ACI J.*, **66**, 1008-1019.
- Khennane, A. and Baker, G. (1992), “Thermoplasticity model for concrete under transient temperature and biaxial stress”, *Proc. R. Soc. Lond., Series A*, **439**, 59-80.
- Khennane, A. and Baker, G. (1993), “Uniaxial model for concrete under variable temperature and stress”, *J. Eng. Mech., ASCE*, **119**(8), 1507-1525.
- Khoury, G. A., Grainger, B.N. and Sullivan, P.J.E. (1985a), “Transient thermal strain of concrete: literature review, conditions within specimen and behaviour of individual constituents”, *Mag. Concr. Res.*, **37**(132), 131-144.
- Khoury, G. A., Grainger, B.N. and Sullivan, P.J.E. (1985b), “Strain of concrete during first heating to 600°C under load”, *Mag. Concr. Res.*, **37**(133), 195-215.
- Khoury, G. A., Majorana, C.E., Pesavento, F. and Schrefler, B.A. (2002), “Modelling of heated concrete”, *Mag. Concr. Res.*, **54**(2), 77-101.
- Neville, A. M., Dilger, W.H. and Brooks, J.J. (1983), *Creep of Plain and Structural Concrete*, Longman Group Ltd., Essex, England.
- Nielsen, C. V., Pearce, C.J. and Bićanić, N. (2001), “Theoretical model of high temperature effects on uniaxial concrete member under elastic restraint”, *Mag. Concr. Res.*, **54**(4), 239-249.
- RILEM TC 129-MHT (1998), “Part 7: Transient creep for service and accident conditions”, *Mater. Struct., RILEM*, **31**, 290-295.
- Schneider, U. (1986), *Properties of Materials at High Temperatures, Concrete*, 2nd edition, RILEM Technical Committee 44-PHT, Technical University of Kassel, Kassel, Germany.
- Schneider, U. (1988), “Concrete at high temperatures A general review”, *Fire Saf. J.*, **13**, 55-68.
- Tanchev, R., Li, L.Y. and Purkiss, J.A. (2001), “Finite element analysis of coupled heat and moisture transfer in concrete subjected to fire”, *Numerical Heat Transfer, Part A*, **39**, 685-710.
- Terro, M.J. (1998), “Numerical modeling of the behavior of concrete structures in fire”, *ACI Struct. J.*, **95**(2), 183-193.
- Thelandersson, S. (1982), “On the multiaxial behaviour of concrete exposed to high temperature”, *Nucl. Eng. and Design*, **75**, 271-282.
- Thelandersson, S. (1987), “Modeling of combined thermal and mechanical action in concrete”, *J. Eng. Mech., ASCE*, **113**(6), 893-906.
- Thienel, K.-C. (1993), “Festigkeit und Verformung von Beton bei hoher Temperatur und biaxialer Beanspruchung Versuche und Modellbildung”, Ph.D. thesis, Heft 104, IBMB, Technical University of Braunschweig, Braunschweig, Germany (in German).
- Thienel, K.-C. and Rostasy, F. S. (1996), “Transient creep of concrete under biaxial stress and high temperature”, *Cem. Concr. Res.*, **26**(9), 1409-1422.
- Ulm, F.-J., Coussy, O. and Bazant, Z.P. (1999), “The “Chunnel” fire. I: Chemoplastic softening in rapidly heated concrete”, *J. Eng. Mech., ASCE*, **125**(3), 272-282.

## Notation

The following symbols are used in this paper:

$A, B, C$	: constants in bi-linear expression of thermo mechanical coefficient
$C_1, C_2$	: constants in Schneider’s model
$c_1, c_2$	: constants in Schneider’s model
$E$	: modulus of elasticity, depending on temperature and stress
$E_{el}$	: temperature dependent elastic modulus
$E_0$	: modulus of elasticity at room temperature
$f_c^0, f_c^T$	: uniaxial compressive strength at room temperature and at temperature $T$
$f, g$	: functions in Schneider’s model
$f_1, f_2$	: functions describing the degradation of $E_{el}$ with temperature
$i, j$	: indices (=1,2,3)
$K$	: plastic to elastic mechanical strain ratio

$R$	: temperature rate
$s$	: dimensionless stress [= $\sigma / f_c^0$ ]
$T$	: temperature
$T_0$	: room temperature
$t$	: time
$\dot{x}$	: derivative with respect to time
$x'$	: derivative with respect to temperature
$\alpha$	: coefficient of free thermal strain
$\beta$	: coefficient of thermo mechanical strain
$\delta_{ij}$	: Kronecker's delta
$\epsilon^\sigma$	: mechanical strain
$\epsilon_c$	: creep strain
$\epsilon_{sse}$	: steady-state creep strain (isothermal conditions)
$\epsilon_{el}^\sigma$	: elastic mechanical strain
$\epsilon_{pl}^\sigma$	: plastic mechanical strain
$\epsilon_{th}$	: free thermal strain (including shrinkage of cement paste)
$\epsilon_{th}^\sigma$	: thermo mechanical strain
$\epsilon_{tot}$	: total strain
$\phi$	: load induced thermal strain function
$\gamma_1, \gamma_2$	: thermo-mechanical coefficients in Thelandersson's formulation
$\eta$	: coefficient of viscosity
$\nu, \nu_c$	: elastic Poisson's ratio and transient creep Poisson's ratio
$\theta$	: dimensionless temperature [= $(T - T_0)/100^\circ\text{C}$ ]
$\theta^*$	: dimensionless transition temperature in parabolic model
$\sigma$	: stress positive as tension
$\tau$	: dimensionless time [= $Rt / T_0$ ]
<b>NB</b>	